

# The role of vicariance vs. dispersal in shaping genetic patterns in ocellated lizard species in the western Mediterranean

O. S. PAULO,\* J. PINHEIRO,\* A. MIRALDO,\* M. W. BRUFORD,† W. C. JORDAN‡ and R. A. NICHOLSS§  
\*Centro de Biologia Ambiental/Departamento de Biologia Animal, Faculdade de Ciências da Universidade de Lisboa, P-1749-016 Lisboa, Portugal, †Cardiff School of Biosciences, Cardiff University, Cathays Park, Cardiff CF10 3TL, UK, ‡Institute of Zoology, Zoological Society of London, London NW1 4RY, UK, §School of Biological Sciences, Queen Mary University of London, London E1 4NS, UK

## Abstract

The schism between North Africa and Southern Europe caused by the opening of the Strait of Gibraltar and the consequent refilling of the Mediterranean basin at the end of Messinian salinity crisis (MSC), 5.33 million years ago, has been advocated as the main event shaping biogeographical patterns in the western Mediterranean as exemplified by the distribution of species and subspecies and genetic variation within the ocellated lizard group. To reassess the role of the MSC, partial sequences of three mitochondrial DNA genes (cytochrome *b*, 12S and 16S ribosomal RNA) and two nuclear genes ( $\beta$ -fibrinogen and *C-mos*) from species of the ocellated lizard group were analysed. Three alternative hypotheses were tested: that divergence was initiated (i) by post-MSC vicariance as the basin filled, (ii) when separate populations established either side of the strait by pre-MSC overseas dispersal, and (iii) by post-MSC overseas dispersal. The pattern and level of divergence detected clearly refute the post-MSC vicariance hypothesis, and support a model of divergence initiated by earlier overseas dispersal. Indeed, our best estimate is that the basal Euro-African divergence predates the MSC event by several million years. The estimated divergence times among the populations in former Miocene Mediterranean islands, the current Betic and Rifian mountains, from adjacent mainland populations suggest overseas dispersal for the former and overland dispersal, or perhaps vicariance, for the latter. These results suggest that the MSC may have played a much less important role in shaping the current western Mediterranean biogeographical patterns than might have been anticipated from the dramatic nature of the episode.

*Keywords:* *Lacerta*, mitochondrial DNA, nuclear genes, phylogeny, Strait of Gibraltar

Received 26 August 2007; revision accepted 11 January 2008

## Introduction

Vicariance and dispersal are the two processes that may have shaped current biogeographical patterns. The first process involves the disjunction of a previously continuous population by the formation of a barrier preventing further contact; the second occurs when a species crosses a pre-existing barrier and successfully colonizes the new area on the other side, resulting in distributional isolation. The relative contribution of each process to current biogeographical patterns is still a matter of debate, especially

because few empirical studies employing molecular phylogenies address this problem (Avice 2000).

Since the discovery of the Late Miocene desiccation of the Mediterranean, known as the Messinian salinity crisis (MSC) (Hsü *et al.* 1973), vicariance has become a common explanation for the biogeography of the western Mediterranean region. This region comprises two distinct parts: North Africa (from Morocco to Tunisia), and the northern shore of the Mediterranean Sea (from the Iberian Peninsula through France to Italy) (Fig. 1). Similar habitats exist on both sides of the region, and a considerable number of conspecific populations or sister species occupy them. Both sides were connected during the MSC, from 5.9 to 5.3 million years ago (Ma) when the Mediterranean Sea dried

Correspondence: Octávio S. Paulo, Fax: 351 217500028;

E-mail: octavio.paulo@fc.ul.pt

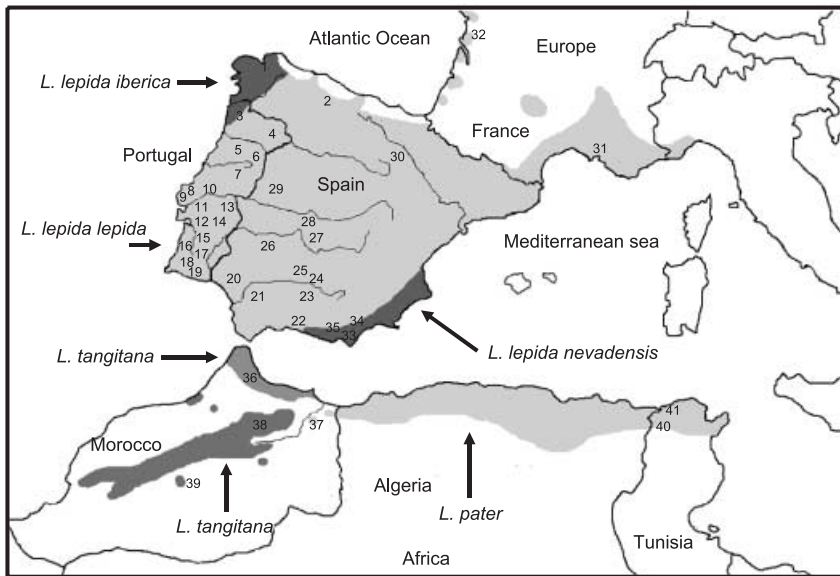


**Fig. 1** Map of the western Mediterranean region. Different grey shades show the distribution of the species and subspecies. Numbers indicate the sites that were sampled.

almost completely, and extensive land-bridges allowed the dispersal of fauna all over the basin. With the opening of the modern Strait of Gibraltar, 5.33 Ma, the refilling of the Mediterranean Sea fragmented the formerly wide-ranging species into several isolated populations on both sides of the strait and on the Mediterranean islands (e.g. Corsica, Sardinia and the Balearics). The vicariance model proposes that, since that time, these isolated populations have diverged and many have become sister species. Several authors had invoked this vicariance event to explain the biogeography of a wide range of species with low dispersal capabilities (e.g. [Busack 1986](#); [Gantenbein & Largiader 2003](#); [Fromhage et al. 2004](#); [Veith et al. 2006](#); [Albert et al. 2007](#)). However, more recent studies show different genetic patterns, which could be better explained by various alternative biogeographical hypothesis, rather than a direct effect of vicariance at the end of the MSC (e.g. [Harris et al. 2002](#); [Paulo et al. 2002b](#); [Carranza et al. 2006](#)).

#### *The ocellated lizards*

The ocellated lizard group has a distribution that includes almost all of the Iberian Peninsula, southern France and northwestern Italy in Europe, and Morocco, northern Algeria and Tunisia in North Africa (Fig. 1). Initially considered as only one species, the North African populations have recently been acknowledged as two different species, *Lacerta pater* in Tunisia/Algeria and *Lacerta tangitana* in Morocco ([Mateo et al. 1996](#)), separated by the Moulouya valley in Morocco. Within Europe, it is generally accepted that there is one species with four subspecies: *Lacerta lepida iberica*, in northern Spain, *Lacerta lepida oteroi*, on the island of Salvora, northern Spain (not shown in Fig. 1), *Lacerta*

*lepida nevadensis*, in the Betic mountains, and *Lacerta lepida lepidota*, that occupies all other areas, from coastal Portugal to the Atlantic and Mediterranean coast of France ([Mateo & Castroviejo 1990](#); [Mateo et al. 1996](#); [Castroviejo & Mateo 1998](#)) (Fig. 1). A residual population was found recently in western Sahara ([Mateo et al. 2006](#)) (not shown in Fig. 1).

For some authors (e.g. [Arnold et al. 2007](#)), this set of *Lacerta* species is already considered to belong to the new genus *Timon*.

A vicariance model for the origin of species of ocellated lizards has been developed based on genetic surveys of allozyme loci. In [Busack's \(1986\)](#) study, Nei's genetic distance among populations in Spain and Morocco was 0.13 (at that time they were considered to comprise a single species, *Lacerta lepida*). [Busack \(1986\)](#) suggested that continued migration between the two sides of the strait after the MSC was the main reason for such a low genetic distance. [Mateo et al. \(1996\)](#) carried out a much more extensive study, and detected much higher values of Nei's genetic distance (0.30–0.37), between the Moroccan *L. tangitana* and the Iberian *L. lepida*, and values of 0.51–0.58 between the latter and the Algerian/Tunisian *L. pater*. Based on these values, the authors estimated a time of vicariance at around 5.5 Ma, approximately coinciding with the end of the MSC. The discrepancies between the two studies could be the result of different sampling strategies.

#### *Kinematics of the western Mediterranean*

Figure 2 shows a very simplified version of the kinematics of the western Mediterranean region, which provides a helpful framework in developing biogeographical models for the ocellated lizards. A more detailed description of

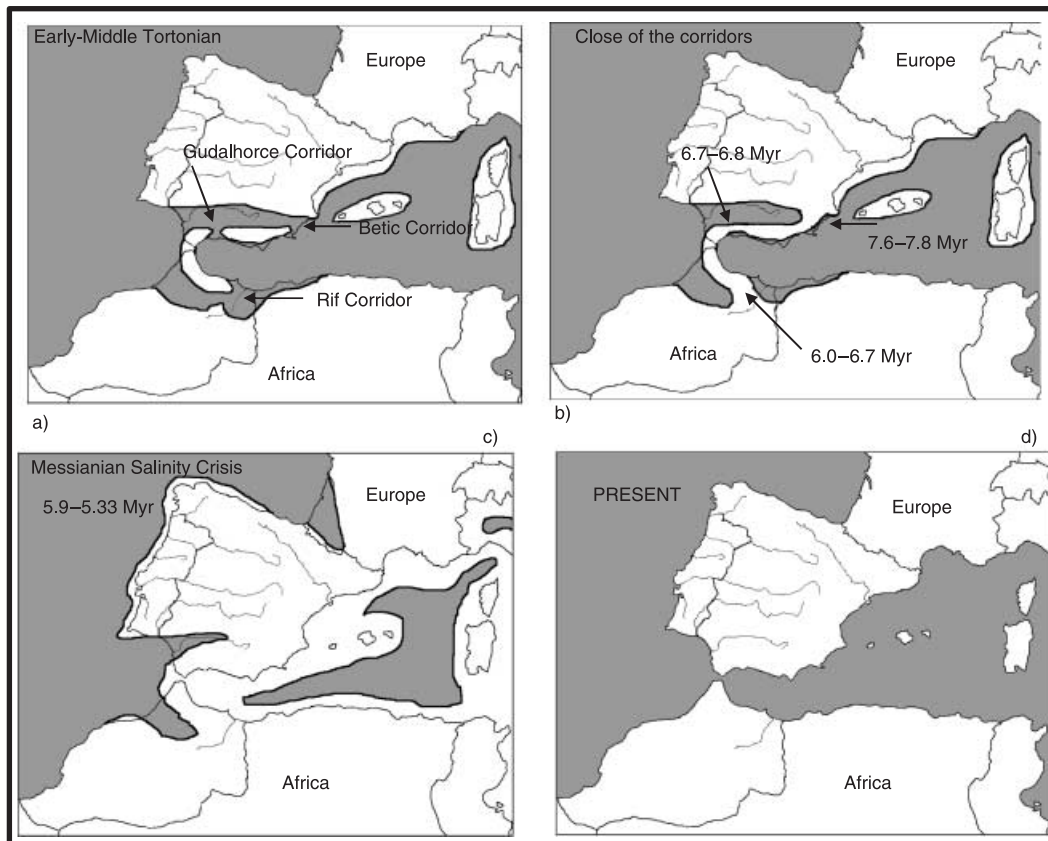


**Fig. 2** A simplified schematic of the evolution of the western Mediterranean region from the middle-Tortonian age until present. (a) Middle-Tortonian age, arrows indicate the three corridors between Mediterranean and the Atlantic Ocean, with islands corresponding to the Betic and Rifian zone. (b) Close of the corridors, with estimated closing times of the three corridors. (c) Messinian salinity crisis, 5.9–5.33 Ma, a period of wide land connections between Africa and Europe. (d) Present-day situation. For the Balearic and Corsica-Sardinia, the representation is not as accurate as for the Betic-Rif zone. See the Kinematics of western Mediterranean section for further explanation.

the events has been given by several authors (e.g. Esteban *et al.* 1996). During the Tortonian, a set of islands existed between the Iberian mainland and northwest Africa (Fig. 2a), partially corresponding to the present day Betic Cordillera in southeastern Iberia, and the Rifian mountains in north Morocco. Figure 2(a) is a 'frozen' moment in a continuous process from the formation of the islands to the progressive reduction of the seaways from deep sea to shallow waters, a process that took several million years and started before the Tortonian (Braga *et al.* 2003).

During the middle-Tortonian, the main seaways between the Atlantic Ocean and the Mediterranean Sea were the Betic and the Guadalorce corridors in the north, and the Rifian corridor in the south (Fig. 2a). The original Betic corridor closed around 10 Ma but the seaways were maintained through an area known as the internal Betics. By the Late Tortonian (7.8–7.6 Ma) this corridor closed on its eastern side (Fig. 2b), allowing a land-bridge between the Betic island and the adjacent mainland (Krijgsman *et al.* 1999, 2000). Later, around 6.7–6.8 Ma, the Guadalorce

corridor closed (Martin *et al.* 2001) (Fig. 2b) and immediately afterwards, between 6.0 Ma and 6.7 Ma, a similar land-bridge was formed on the southeastern side of the Rifian corridor (Fig. 2b) (Krijgsman & Langereis 2000).

The beginning of the MSC has been dated at  $5.96 \pm 0.02$  Ma: it caused extensive land-bridges to form between Africa and Europe, and among the former Miocene islands through the Gibraltar region (Fig. 2c) (Krijgsman *et al.* 1999). The MSC ended abruptly at 5.33 Ma with the opening of the Strait of Gibraltar and the reestablishment of marine conditions in the Mediterranean (Duggen *et al.* 2003). Consequently, land connections between Iberia and Africa disappeared, but the former Miocene islands have remained extensively connected with the adjacent mainland to the present (Fig. 2d).

#### *Alternative biogeographical hypotheses*

The aim of this study was to test three major alternative hypotheses for the differentiation of the ocellated lizard

group of species, and consequently, to draw more general lessons about the role of post-MSC vicariance in producing the phylogeographical patterns of the western Mediterranean region:

*Post-MSC vicariance.* This was the original hypothesis suggested by Busack (1986). It proposes that differentiation between North African and European populations of *Lacerta* started at the end of the MSC (5.33 Ma) just after the opening of the Strait of Gibraltar. It predicts that a phylogeny for *Lacerta* in this region would have two major lineages, corresponding to groups on either side of the Strait of Gibraltar. Well-differentiated sublineages would be possible, but this hypothesis does not predict that the geographical position of the sublineages would correspond to former Miocene islands. It assumes that originally, the species occupied just one of the mainlands and that during the MSC it used the land-bridges to cross between mainlands and around the end of MSC, they started to differentiate.

*Pre-MSC overseas dispersal.* Under this hypothesis, the extent and pattern of genetic divergence among the ocellated lizards was due to dispersal by sea between the two continents before the beginning of the MSC (5.9 Ma). The splitting could have been initiated by colonization in one direction or other across the Mediterranean Sea, and subsequent differentiation.

An extension of this hypothesis assumes that if pre-MSC overseas dispersal was the key process by which areas could be colonized, then the former Miocene islands could also have been colonized by overseas dispersal before they were connected to adjacent mainland areas. If so, up to four well-differentiated lineages corresponding to the two mainland areas and the two former Miocene islands should be detected. As all major dispersal events would have occurred before both the MSC and the formation of land-bridges between former Miocene islands and adjacent mainland, the divergence time would therefore be greater than 7.8 Ma for the Betic populations and greater than 6.7 Ma for the Rifian populations. Any sequence of island and mainland colonization events (i.e. any set of relationships among lineages) would be consistent with this scenario.

An alternative extension of the hypothesis assumes that the former Miocene islands would have been colonized by dispersal along land bridges to the Betic and Rifian peninsulas from adjacent mainland populations. This history would have produced four different lineages, with two pairs of mainland/peninsula sister taxa. The divergences times inside each these two pairs should then be around the estimated time for formation of land-bridges between former islands and adjacent mainland. That is, 7.8–7.6 Ma for the Betic–Iberia land-bridge, and 6.7–6.0 Ma for the Rifian–Morocco land-bridge.

*Post-MSC overseas dispersal.* Under this hypothesis, the divergence from North Africa and Europe started after the end of MSC and by the result of overseas dispersal across the Mediterranean from one of the sides. Under this scenario, the level of divergence across the Strait of Gibraltar should be more recent than 5.3 Ma, and no particular pattern of intracontinental differentiation is postulated.

## Materials and methods

### Sampling, extraction and DNA sequencing

Samples were collected by clipping two or three tail rings of free-living animals that were immediately released back into the wild. Figure 1 shows the location of the 41 sample sites and Table 1 identifies the 75 samples analysed. Total DNA extraction was carried out according to standard protocols. Polymerase chain reaction (PCR) amplifications were performed for parts of three different mitochondrial DNA [(mtDNA); cytochrome *b*, 16S and 12S ribosomal RNA (rRNA)] and two nuclear DNA [(nDNA);  $\beta$ -fibrinogen and C-mos] genes. The amplifications were carried out with the general primers: 12S rRNA–L1019 5'-CAAACCTGGATT-AGATACCCCACTAT-3' and H1478 5'-TGAAGTGCAGAGGGTGACGGGCGGTGTGT-3'; 16S rRNA–L02510 5'-CGCCTGTTTATCAAAAACAT-3' and H03063 5'-CTCCG-GTTTGAAGTCAAGATC-3'; cytochrome *b* the truncated version of primer L14841, 5'-CCATCCAACATCTCAGC-ATGATGAAA-3' and H15551 5'-AAATAGGAAGTATCAC-TCTGGTTT-3'. Two cytochrome *b* internal primers were also designed and used to sequence fragments of the amplified product: L15174 5'-TGAGGACAAATATCATTT-TGAGGCGC-3' and H15146 5'-GATATTTGTCTCAGGG-3'. For the amplification of intron 7 of the nDNA gene  $\beta$ -fibrinogen the primers FIB-BI7U and FIB-BI7L (Prychitko & Moore 1997) were used and for the C-mos gene the primers Mos-F and Mos-R (Godinho *et al.* 2006) were used.

PCRs were performed in a final volume of 50  $\mu$ L, with 2  $\mu$ L of DNA (50–100 ng), 50 pM of each primer, 1.25 mM of each dNTP, in a reaction buffer of 50 mM KCl, 20 mM Tris-HCl (pH 8.4), 2 mM MgCl<sub>2</sub> with 10  $\mu$ g BSA and 1 U *Taq* DNA polymerase (GibcoBRL). A programmable thermal-cycler (Perkin-Elmer models 9600, 2400 and 2700) was used for amplifications. PCR conditions were as follows: an initial denaturation step of 94 °C for 5 min followed by 30 cycles consisting of denaturation at 94 °C for 30 s, annealing at 51 °C for 30 s for mtDNA genes and 57 °C for nuclear genes, extension at 72 °C for 30 s, and a final extension step of 72 °C for 7 min. The DNA was then purified and concentrated with GeneClean (Bio 101). An aliquot of 25–50  $\mu$ g of purified DNA template was used in dRhodamine BigDye terminator cycle sequencing following the manufacturer's instructions. Both strands of PCR products

**Table 1** Sampled localities with the respective name and country of origin. For each locality, the respective species and subspecies name is presented (LLL, *Lacerta lepida lepida*; LLI, *Lacerta lepida iberica*; LLN, *Lacerta lepida nevadensis*; LT, *Lacerta tangitana*; LP, *Lacerta pater*; LAG, *Lacerta agilis*; LSC, *Lacerta schreiberi*). Also for each locality, the cytochrome *b* (Cyt *b*) haplotype numbers are shown from H1 to H55. For the selected samples, sequences for the partial fragments of the other four genes analysed, together with the respective GenBank Accession numbers, are shown

Taxa	Country	Location	Location no.	Cyt <i>b</i> haplotype no.	GenBank Accession nos				
					Cyt <i>b</i>	12S	16S	C-mos	β-fibrinogen
LLL	Spain	Pontes Rodrigo	26	H1	AF378968				
LLL	Spain	Navahermosa	28	H1	AF378968				
LLL	Spain	Soria	30	H1	AF378968				
LLL	France	Crau	31	H1	AF378968				
LLL	France	Oleron	32	H1	AF378968				
LLL	Portugal	Arrábida	12	H2	AF378969				
LLL	Portugal	Évora	14	H3	AF378970	AF378942	AF378954	EU365407	EU365428
LLL	Spain	Sierra Madrona	24	H4	AF378971				
LLL	Spain	Sierra Madrona	24	H5	AF378972				
LLL	Spain	Sierra Morena	25	H6	AF378973				
LLL	Spain	Montes Toledo	27	H7	AF378974				
LLL	Spain	Montes Toledo	27	H8	AF378975				
LLL	Spain	Andalucia	23	H9	AF378976				
LLL	Spain	Andalucia	20	H10	AF378977				
LLL	Spain	Andalucia	22	H11	AF378978				
LLL	Spain	Andalucia	21	H12	AF378979				
LLL	Portugal	Moura	15	H13	AF378980				
LLL	Portugal	Estuário do Tejo	11	H14	AF378981				
LLL	Portugal	São Mamede	13	H15	AF378982				
LLL	Portugal	Peniche	8	H16	AF378983				
LLL	Portugal	Peniche	8	H17	AF378984				
LLL	Portugal	Samarra	9	H17	AF378984				
LLL	Portugal	Samarra	9	H18	AF378985				
LLL	Portugal	Paul Boquilobo	10	H19	AF378986				
LLL	Portugal	Serra da Estrela	7	H20	AF378987	AF378942	AF378948	EU365407	EU365429
LLL	Portugal	Serra da Estrela	7	H21	AF378988				
LLL	Portugal	Ilha Velha	8	H21	AF378988				
LLL	Spain	Bejar	29	H22	AF378989	AF378942	AF378953	EU365407	EU365424
LLL	Spain	Bejar	29	H23	AF378990				
LLL	Spain	Bejar	29	H24	AF378991	AF378942	GB000000	EU365407	EU365425
LLL	Spain	Navahermosa	28	H25	AF378992				
LLL	Portugal	Serra Liomil	5	H26	AF378993				
LLL	Spain	Asturias	2	H27	AF378994				
LLL	Portugal	Montezinho	4	H27	AF378994				
LLI	Spain	Galicia	1	H28	AF378995	AF378942	AF378951	EU365407	EU365430
LLI	Spain	Galicia	1	H29	AF378996				
LLI	Portugal	Gerês	3	H30	AF378997				
LLI	Portugal	Gerês	3	H31	AF378998				
LLL	Portugal	Montezinho	4	H32	AF378999	AF378942	AF378951	EU365407	EU365431
LLL	Portugal	Montezinho	4	H33	GB000000				
LLL	Portugal	Foz Coa	6	H34	AF379000				
LLL	Portugal	Grandola	16	H35	AF379001				
LLL	Portugal	Grandola	16	H36	AF379002				
LLL	Portugal	Mertola	17	H37	AF379003				
LLL	Portugal	Castro Marim	19	H37	AF379003	AF378943	AF378951	EU365407	EU365426
LLL	Portugal	Castro Verde	18	H38	AF379004				
LLL	Portugal	Castro Verde	18	H39	AF379005	AF378943	AF378951	EU365407	EU365427
LLL	Portugal	Castro Marim	19	H39	AF379005				
LLN	Spain	Sierra Filabres	34	H40	AF379006	AF378944	AF378949	EU365408	EU365423
LLN	Spain	Sierra Filabres	34	H41	AF379007				
LLN	Spain	Sierra Filabres	34	H42	AF379008				

Table 1 Continued

Taxa	Country	Location	Location no.	Cyt <i>b</i> haplotype no.	GenBank Accession nos				
					Cyt <i>b</i>	12S	16S	C-mos	$\beta$ -fibrinogen
LLN	Spain	Sierra Filabres	34	H43	AF379009				
LLN	Spain	Sierra Filabres	34	H44	AF379010	AF378941	AF378950	EU365408	EU365421
LLN	Spain	Almeria Zurgena	33	H45	AF379011				
LLN	Spain	Turon	35	H46	AF379012	AF378941	AF378952	EU365408	EU365422
LP	Tunisia	Tabarka	41	H47	AF378963	AF378947	AF378958	EU365409	EU365415
LP	Tunisia	Tabarka	41	H48	AF378964	AF378942	AF378958	EU365409	EU365414
LP	Tunisia	Tabarka	41	H49	AF378965				
LP	Tunisia	Tabarka	40	H50	AF378966				
LP	Tunisia	Tabarka	40	H51	AF378967	AF378947	AF378958	EU365409	EU365413
LT	Morocco	Xauen	36	H52	AF378961	AF378945	AF378955	EU365410	EU365419
LT	Morocco	Xauen	36	H53	AF378962	AF378945	AF378955	EU365410	EU365420
LT	Morocco	Debdou	37	H54	AF378960	AF378945	AF378956	EU365410	EU365418
LT	Morocco	Azrou	38	H55	AF378959	AF378946	AF378957	EU365409	EU365416
LT	Morocco	Azrou	38	H55	AF378959	AF378946	AF378957	EU365409	EU365417
LT	Morocco	Ouarzazate	39		AF080294	AF149947	AF149963		
LAG	Spain				AF373032	AF080293	AF080295	EU365405	EU365411
LSC	Portugal				AF372121	AF206591	AF206591	EU365406	EU365412

were sequenced. Products of sequencing reactions were analysed on a semiautomatic genetic analyser (ABI PRISM models 377 and 310).

#### Analytical approach

DNA sequences were initially aligned using CLUSTAL\_X version 1.8 (Thompson *et al.* 1997) and the resulting alignment was then inspected and manually changed to eliminate a few frame shifting gaps. Gaps were treated as missing data. Sequences from two closely related species, *Lacerta schreiberi* and *Lacerta agilis*, were used as outgroups. Three additional GenBank sequences from *Lacerta tangitana* (Table 1 and location 39 in Fig. 1) were used to confirm their position in the phylogenetic trees.

The effect of saturation on the substitution rate in cytochrome *b*, the most rapidly evolving fragment, was investigated by plotting transitions at the third positions of each codon against uncorrected genetic distances and by plotting uncorrected distances against Kimura 2-parameter distances. In both cases, an asymptotic curve implies saturation. For the nuclear genes, nucleotide ambiguities of similar peak size in chromatograms were considered as evidence of potential heterozygous sites. The IUPAC ambiguity code was used for subsequent analyses.

Phylogenetic analysis was performed using PAUP\* version 4.0.b4a (Swofford 2000). MODELTEST 3.7 software (Posada & Crandall 1998) associated with PAUP\* was used to select the most appropriate evolutionary model for the different data sets according to the Akaike information criterion (AIC). The most appropriate model for each case

was then used to calculate the maximum-likelihood (ML) phylogenetic tree. The neighbour-joining (NJ) tree for each data set was also calculated with the previously selected model of sequence evolution. This calculation involved the following parameters: (i) a shape parameter of the gamma distribution used to set the relative size of four rate categories, (ii) the proportion of invariable sites, and (iii) the proportions of the two types of transition and four types of transversion (or the transition/transversion ratio in simpler models). The data was resampled 1000 times using the nonparametric bootstrap technique to evaluate the robustness of the nodes of the phylogenetic trees. The Shimodaira–Hasegawa test (Shimodaira & Hasegawa 1999) was implemented, when necessary, to test alternative tree topologies. The a priori-selected topology for the test is the one implied in all our hypotheses, the one assuming a basal African-European split and monophyletic groups in each continent. This tree was then compared with other topologies. Analyses were carried out for separate and combined data sets after testing for incongruence. The incongruence length difference test (ILD) (Farris *et al.* 1995), was implemented in PAUP\* with all invariant characters removed.

To assess if the sequences evolved in a clock-like manner, a likelihood ratio test (LRT) was performed. The log-likelihood value of a tree with the same topology and evolutionary model was calculated with and without enforcing a molecular clock. Twice the difference between the likelihoods was then compared with a  $\chi^2$  distribution with  $n-2$  degrees of freedom, where  $n$  is the number of sequences used in the analysis (Huelsenbeck & Crandall 1997).

Unweighted parsimony (UP) analyses were also carried out using PAUP, on all data sets. The optimal tree was found by a heuristic search with tree-bisection–reconnection as the branch-swapping algorithm. Initial trees were obtained via stepwise addition with 100 replicates of random addition sequence. Again, bootstrapping with 1000 pseudo-replicates was performed to evaluate the robustness of the nodes of the phylogenetic trees.

Bayesian (BA) analyses were undertaken using MRBAYES version 3.1 (Ronquist & Huelsenbeck 2003). The posterior probabilities of the phylogenetic trees were estimated by a Metropolis-coupled, Markov chain Monte Carlo sampling algorithm (MCMCMC). The Markov chain Monte Carlo (MCMC) procedure ensures that trees are sampled in proportion to their probability of occurrence under the given model of gene-sequence evolution while the MCMCMC approach ensured that the Markov chain did not become trapped in local optima. After some trial runs, the conditions for the Bayesian analysis were set up to ensure that the likelihood scores of the trees reached stationarity over the course of the sampling. For each analysis, a total of  $2 \times 10^6$  samples were taken, with successive samples separated by 100 generations (iterations of the sampling process) with a 'burn-in' period covering the first 5%, so that the samples were independent of the starting conditions.

For analysis of combined data, model selection was carried out separately for each mtDNA data set with MRMODELTEST version 2.2 (Nylander 2004) and implemented according to the author's recommendations. A combined matrix of the three mitochondrial genes was set up and the previously selected models were used to analyse the data (Nylander *et al.* 2004). Different partitions were allowed to evolve at different rates, with unlinked topology and unlinked parameters for the nucleotide substitution models across partitions. For each model, the runs were carried out using different random starting seed. These runs were assessed for congruence of the likelihood values (Huelsenbeck *et al.* 2002). The likelihood values for each of the analyses were compared and the best used to determine the topology branch length and clade robustness through the clade credibility values obtained from a 50% majority-rule consensus tree of the retained 95% trees. These analyses were repeated for all data sets. For the cytochrome *b* data, a Bayesian analyses was also performed with a codon partition according to the site's position.

Finally, several analyses for estimating divergence times among clades were carried out with BEAST version 1.4.1 (Drummond & Rambaut 2003) and data on cytochrome *b*. The details of the provisional calibration rates are presented in Paulo (2001). The most appropriate published cytochrome *b* sequence data sets for calibration of a reptile-specific molecular clock were those from two studies on Canary Islands reptiles (Thorpe *et al.* 1994; González *et al.*

1996). The calibrations were performed using GenBank sequences (Accession numbers are listed in the two studies of Thorpe *et al.* and Gonzales *et al.*). The geological date of origin of the most recently emerged Canary Island, El Hierro, was used for calibration. The rate estimates were based on an assumption of immediate colonization after island formation. Consequently, the true values may be higher. When both *Gallotia* data sets were analysed together, the rate was approximately 2% pairwise sequence divergence with a standard deviation of 0.54, coinciding with the value of the provisional 'standard' molecular clock for birds and mammals. Based on this information, three rates were adopted: (i) the standard rate; (ii) a slow rate of 1.7%, assuming a slightly longer generation time and larger body size for *Lacerta* group than for the two *Gallotia caesaris* subspecies studied (Paulo 2001); and (iii) a fast rate of 2.5% assuming an underestimation of the mean calibration rate. These rates correspond to the three different mutation rates 0.01, 0.0085 and 0.0125 mutations/site/million years implemented in BEAST.

For the cytochrome *b* data set, codon-based models with either a strict or relaxed molecular clock were implemented, assuming for the latter model that rates were lognormally autocorrelated among branches (Drummond *et al.* 2006). Runs with  $10^6$  generations and a burn-in of 10% were initially implemented and, after inspection of the effective sample size (ESS) and convergence, adjustments were made to the number of generations and the optimization procedures in order to have ESS above 100 and convergence and stability for all the relevant statistics. Combinations of divergence time estimates from the different mutation rates were performed in TRACER version 1.3 (Rambaut & Drummond 2003).

## Results

### *Levels of variability*

Initially, 75 samples were sequenced for the cytochrome *b* gene (Table 1). After preliminary analysis of these sequences, 19 samples from the main clades were selected and sequenced for fragments of the other mtDNA and nDNA genes (Table 2). A total of 55 unique cytochrome *b* haplotypes, 12 different 16S rRNA haplotypes, seven 12S rRNA haplotypes, 19 different  $\beta$ -fibrinogen sequences (with eight of the sequences showing potential heterozygous sites) and four C-mos sequences were obtained (any showing potential heterozygous sites were found; Table 1). Each of potential heterozygous sites of the  $\beta$ -fibrinogen sequences was usually restricted to a single identified clade.

No gaps or premature stop codons were identified in the cytochrome *b* sequences, and all therefore represented uninterrupted open reading frames, suggesting that they were functional. When ambiguous alignments were

**Table 2** Variability and phylogenetic model details for each gene and 1015 gene combination analysed: fragment size in base pairs, numbers of variable and parsimony informative sites, selected evolutionary model, shape parameter of the gamma distribution ( $\Gamma$ ), proportion of invariable sites (I), transition-transversion rate (Ti/Tv), individual substitution rates and number and length of underweighted parsimony (UP) trees. \*There is not enough information in the data about certain substitutions rates; consequently, the model is not shown

Fragment	Size (bp)	Variable Informative		Model	$\Gamma$	I	Ti/Tv	A-C	G-A	A-T	C-G	C-T	No. of UP trees (length)
		sites	sites										
mtDNA													
12S rRNA	423	52	35	GTR + $\Gamma$	0.0998			1.0354	5.5164	2.4875	0.0001	16.2737	6 (67)
16S rRNA	553	92	62	GTR + $\Gamma$	0.1225			3.1114	6.3682	2.2182	0.0001	20.3486	5 (127)
Cytochrome <i>b</i>	663	240	195	TVM + I		0.6013		7.0438	58.5034	6.9503	3.5492	58.5034	2 (509)
Three mtDNA genes	1639	375	288	GTR + $\Gamma$	0.1481			4.8796	16.2934	5.3054	1.3706	51.1896	4 (654)
Nuclear													
$\beta$ -fibrinogen	656	51	20	HKY + $\Gamma$	0.2587		2.0519						400 (57)
C-mos	534	15	11		*								3 (18)
Two nuclear	1190	66	31	HKY + $\Gamma$		0.8136	2.1011						24 (75)
mtDNA + nuclear													
All genes	2829	441	319	GTR + $\Gamma$ + I	1.2691	0.7186		4.3703	11.386	3.5898	1.2856	38.1479	4 (734)

produced for the 12S rRNA and 16S rRNA genes, several slightly different alignments including the removal of the ambiguous positions or indels, were analysed, without producing any major differences in the results. For the nuclear genes, the alignment was straightforward for C-mos but the  $\beta$ -fibrinogen gene showed some short indels, but none were heterozygotic for length variation. Based on these alignments, the best models of sequence evolution were determined for each sequence and sequence combination (Table 2).

### Cytochrome *b*

No evidence for saturation was detected in the ocellated lizard cytochrome *b* sequences. The relevant statistics and evolutionary model selected are shown in Table 2. Under the TVM + I model (Table 2), two trees were obtained by ML. The optimal topology obtained was tested against a constrained tree in accordance with the a priori hypothesis of a basal Euro-African and a monophyletic group on each mainland. A Shimodaira–Hasegawa test showed no statistical significant difference ( $P = 0.379$ ) between the optimal tree ( $-\ln L$  3264.14881) and a tree with the topological constrain ( $-\ln L$  3264.91804). The main difference between the optimal tree and the constrained one shown in Fig. 3, was the position of clade N which was basal to all other clades in the optimal tree and not a sister group of clade L as in Fig. 3.

Trees produced by the NJ, UP and BA approaches all showed similar results to that of ML; bootstrap values and clade credibility values are shown in Fig. 3.

Finally, for TVM + I model, the LRT showed a statistically significant difference in the log likelihoods of phylogenetic

trees with or without the molecular clock assumed – at the 95% level but not at the 99% ( $2\delta = 76.41018$ , d.f. = 55,  $0.05 < P < 0.01$ ).

### All mtDNA genes

Selected samples representative of the major clades were sequenced for fragments of the 12S rRNA and 16S rRNA mtDNA ribosomal genes. These data sets, as well as, the combination of all three mtDNA data sets (12S rRNA, 16S rRNA and cytochrome *b*) were analysed as above; the relevant statistics and evolutionary model selected are shown in Table 2.

For the combined data set, the incongruence length difference test showed that the fragments were not incongruent (ILD  $P = 0.79$ ). The  $\chi^2$  test of homogeneity of base frequencies across taxa showed no significant difference ( $\chi^2 = 6.88$ , d.f. = 60,  $P = 1.00$ ).

The LRT showed no statistically significant difference between the log likelihoods of phylogenetic trees, with or without the molecular clock assumed ( $2\delta = 21.19$ , d.f. = 17,  $P > 0.05$ ).

Trees inferred with different methods – ML, NJ, UP and BA – produced similar topologies (Fig. 4a), with the exception of three of the four UP trees, where again clade N was basal to all other clades and not a sister group of clade L. The topology of the main clades is similar to that of Fig. 3, only support values differ between them.

### Nuclear genes

For the two nuclear genes  $\beta$ -fibrinogen and C-mos, sequences were obtained from selected samples representative

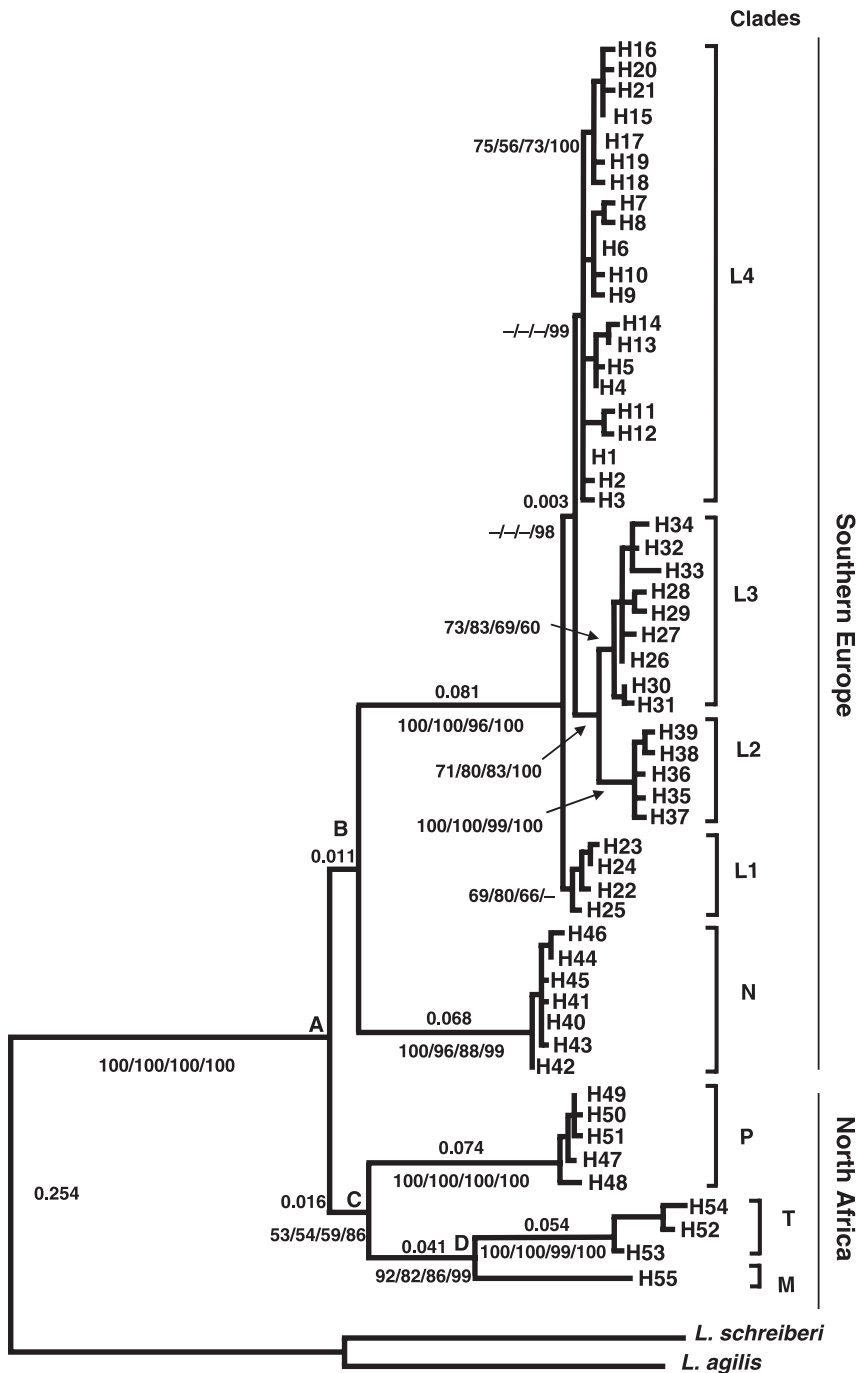


**Fig. 3** Maximum-likelihood phylogenetic tree of 663 bp of the cytochrome *b* gene. Numbers in terminal nodes refer to the haplotype numbers as in Table 1. Main geographical division between Africa and Europe is indicated, and inside each division, the respective species and clades are presented: *Lacerta lepida*, clade L (subclades L1 to L4) and N; *Lacerta tangitana*, clades T and M; *Lacerta pater*, clade P (see text for details). Nodes A to D as in Table 3. Numbers above the branches are branch lengths and numbers below are the bootstrap support values obtained from 1000 pseudoreplicates from maximum parsimony, corrected distance method and maximum likelihood; the fourth number is the Bayesian credibility value.

of the major mtDNA clades. Table 2 gives details for these two genes as well as for the concatenated data set. Due to the low levels of variability in C-mos sequences, no further analysis of this gene alone was performed apart from UP analysis. The main mtDNA clades were identified but mtDNA clades M and P were not resolved.

Figure 4b shows a phylogram with a topology essentially identical to that obtained for  $\beta$ -fibrinogen by ML. The

main difference was that samples of clade N did not group together as in Fig. 4b. This lack of resolution of the basal relationships was also obtained by BA, NJ and UP. Figure 4b shows the robustness values of each node obtained by the different methods.

Figure 4b shows the optimal phylogeny, for the combined nuclear DNA data set, obtained by ML with the selected evolutionary model ( $-\ln L = 2151.44598$ ), which

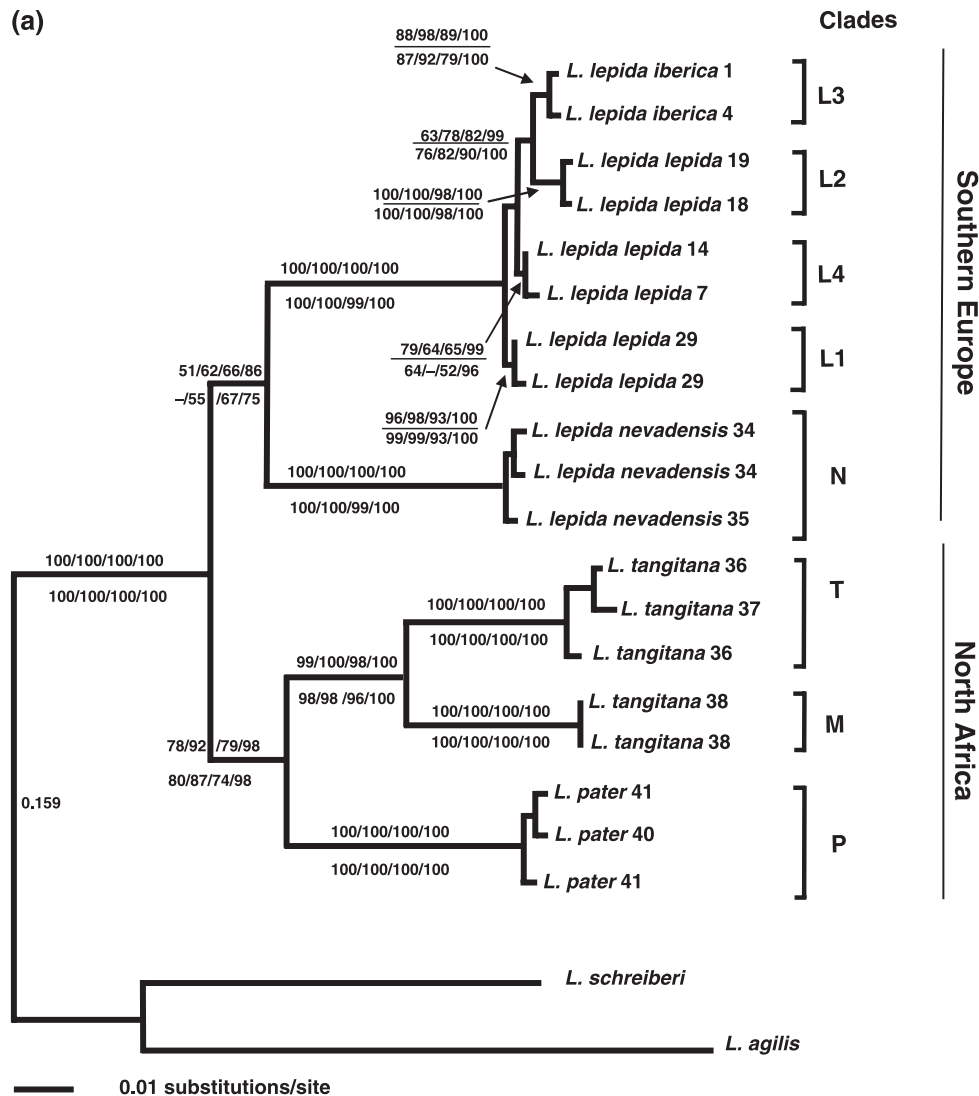


**Fig. 4** (a) Maximum-likelihood phylogenetic tree of 1648 bp of three combined fragments of mtDNA 12S and 16S rRNA genes and the cytochrome *b* gene. (b) Maximum-likelihood phylogenetic tree of 1190 bp of the  $\beta$ -fibrinogen and C-mos fragments. Numbers above and below branches are the bootstrap support values obtained from maximum parsimony, corrected distance method and maximum likelihood; the fourth number is the Bayesian credibility value. In 4a, the numbers above the branches are from the five-fragment data set and below are from the three mtDNA genes. In 4b, the numbers above the branches are from the combined nuclear data set and below are from  $\beta$ -fibrinogen alone. Names in terminal nodes refer to the sample species names and respective locations as in Table 1. For both (a) and (b), the main geographical division between Africa and Europe is indicated, and inside each division, the respective species and mtDNA clades are presented: *Lacerta lepida*, clades L1 to L4 and N; *Lacerta tangitana*, clade T and M; *Lacerta pater*, clade P (see text for details).

also provided the best resolution obtained by any of the inference methods used. Clades are maintained across the methods but the basal relationship among the clades was either identical to Fig. 4b (BA) or had clade L (NJ) or clade P (UP) basal. The combined nuclear data set show consistently higher robustness values for the different methods than the  $\beta$ -fibrinogen alone. However, the relationship among the North African clades remains unresolved and the N–L relation still has weak support.

#### All genes

Finally, the results from the combined analyses of data sets for all five genes are set out in Table 2. The ILD test showed that the fragments were not incongruent ( $P = 0.71$ ). The  $\chi^2$  test of homogeneity of base frequencies across taxa showed no significant difference ( $\chi^2 = 3.88$ , d.f. = 60,  $P = 1.00$ ).

The topology of the optimal phylogeny obtained by ML with the selected evolutionary model is identical to Fig. 4a.

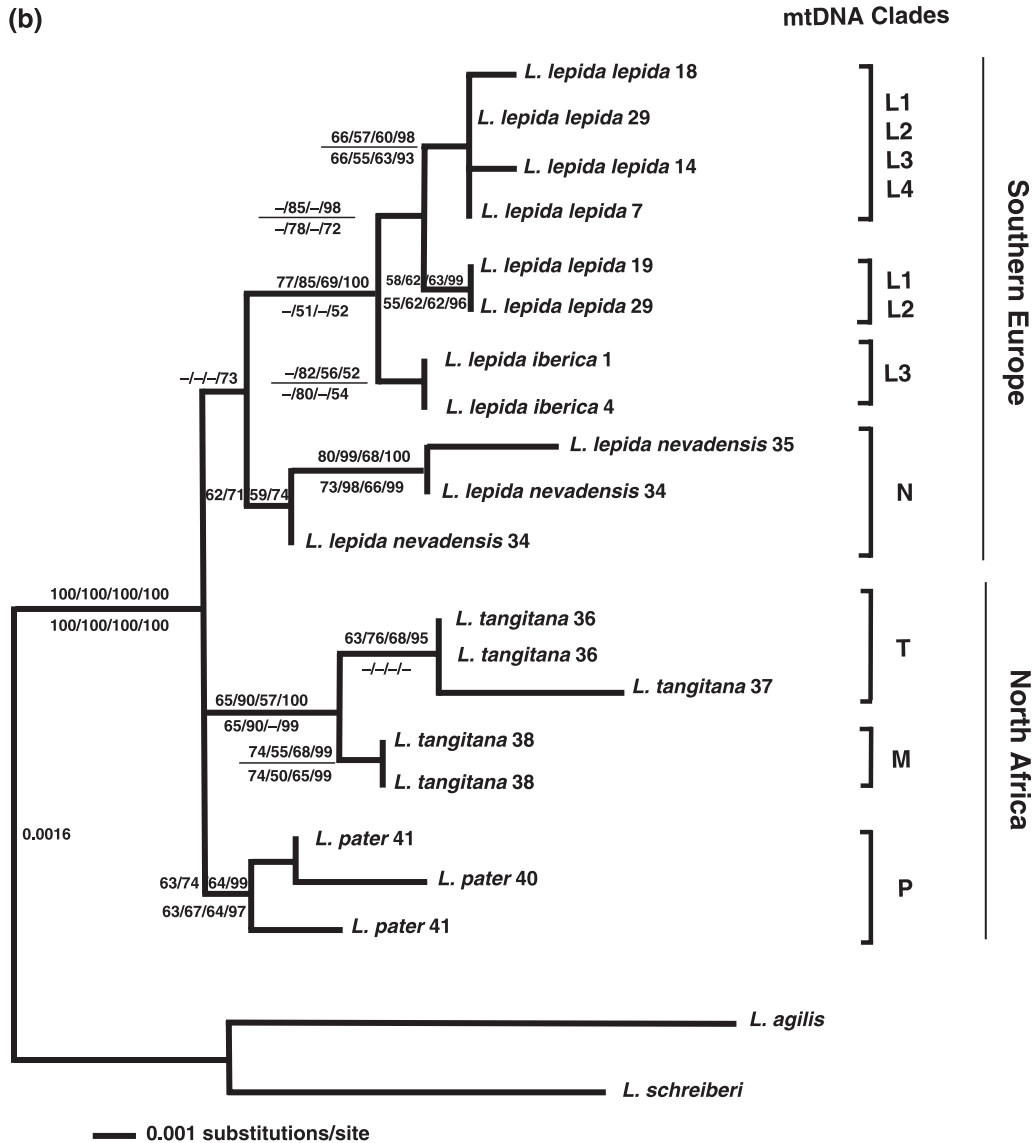


Fig. 4 Continued

The four methods produce the same topology but with different branch support (Fig. 4a)

*Pattern of divergence*

Each of the two main ocellated lizards clades (P, M, T and N, L, see Figs 3 and 4a, b) corresponded to the two main geographical regions occupied by this group of species, i.e. North Africa and Europe (Fig. 5). Both clades were supported by high bootstrap and Bayesian credibility values when the three mtDNA genes or all genes were analysed together (Fig. 4a).

For the cytochrome *b* and the  $\beta$ -fibrinogen gene analyses, the European clade lacked strong support whichever of the four inference methods was used (Figs 3 and 4b). The main reason for these equivocal results was the unstable position

of the N clade: it was sometimes the basal clade in the cytochrome *b* gene analyses or could have an unresolved position in the  $\beta$ -fibrinogen gene analyses. However, when either the mtDNA genes or the nuclear genes or both were analysed together, the European clades have higher support values. The African clade has higher support, especially from the Bayesian credibility values, when cytochrome *b* was analysed alone (Fig. 3) or with the other mtDNA genes, but lacked support when  $\beta$ -fibrinogen was analysed alone or in combination with C-mos, because, consistently, the relationships between the main African subclades (P and M, T) were unresolved (Fig. 4b).

Inside the African clade, the two main subclades corresponded to the species *Lacerta pater* from Algeria/Tunisia (P) and *Lacerta tangitana* from Morocco (M, T) with a discrepancy in northeast Morocco. Inside the Moroccan group,

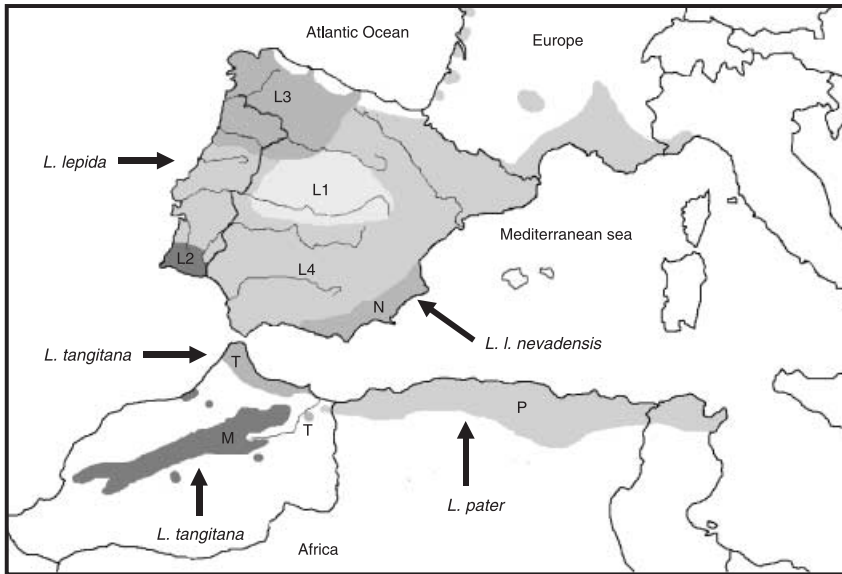


**Fig. 5** Map of the western Mediterranean region. Grey colours show the putative distribution of the clades identified in Fig. 3 (same code as in Fig. 3).

additional divergence was found between sequences from the Atlas mountains (M) and those from the Rif mountains and the north of the country (T), a pattern consistent across the data sets and across all inference methods (Figs 3, 4a, b and 5).

Inside the European clade, there were two other subclades L and N, each one having very high support values across the analysed data sets and across all inference methods (with the exception of the  $\beta$ -fibrinogen data set, which did not provide clear support for the N clade and gave equivocal support for the L clade; Fig. 4b).

The C-mos sequences seemed to support almost all the main clades except the M and P as they have identical C-mos sequences. Clades T and N differed by just a single substitution each, at different sites, from the group 'M, P' while Clade L differed by two substitutions from the 'M, P' sequence at another two different sites.

Inside Iberia, clade N seemed to overlap with the Betic mountains in southeastern Spain. Clade L was divided into several subclades L1–L4 that corresponded to samples from the subspecies *Lacerta lepida lepida* and *Lacerta lepida iberica*. Clade L3 was distributed in the northwest corner of Iberia and overlapped the conventional distribution of *Lacerta lepida iberica*, but extended much more easterly than the subspecies range (Figs 1, 3, 4 and 5). Again, this pattern was consistent across the data sets and across all inference methods, but for the  $\beta$ -fibrinogen gene there was insufficient resolution to differentiate some of these subclades while others seemed to be paraphyletic (Fig. 4b).

#### Divergence time estimates

The divergence times of several nodes (A to D and Iberian clade L splits in Fig. 3 and Table 3) were estimated using

both relaxed and strict molecular clock approaches. The results of the relaxed molecular clock implemented for the cytochrome *b* data set are shown in Table 3. Results of the strict molecular clock approach were very similar but with slightly lower mean values (not shown).

The oldest split between Africa and Europe (node A), corresponding to the oldest cladogenic event inside the ocellated lizards species complex, had a mean estimated value between 9.3 Ma and 13.3 Ma. The range of the 95% highest posterior density (HPD) interval of the divergence times for the combined analysis was from 6.4 to 16.2 Ma.

The two secondary divergences inside each continent (nodes B and C) appeared almost simultaneously. The first African split, between the Tunisian and Moroccan clades (node C), and the second African split (node D) between the Atlas clade and the Rifian clade were separated by 1–4 Ma and were both probably Upper Miocenic events.

The second Iberian split (clade L), was a Plio–Pleistocenic event. The Iberian subclades (L1–L4), show two categories of events with a mean divergence time around 1.5 Ma and under 1.0 Ma (results not shown). A detailed analysis of these Iberian events will be the subject of another paper with further data.

#### Discussion

This set of results show a well-structured and deep phylogeny with a first, and very old, split between the European and the African set of populations. In combined data sets, these two main clades are reciprocally monophyletic; one clade corresponds to two African species – *Lacerta tangitana* and *Lacerta pater* – the other to *Lacerta lepida* in Europe.

**Table 3** Divergence time estimated in million years ago (Ma) for the cytochrome *b* mtDNA gene of ocellated lizard species, for the main five nodes recovered in the phylogenetic analyses (Fig. 3). Divergence times were estimated under three different assumptions of pairwise sequence divergence (2%, 1.7% and 2.5%). For each node, the mean divergence time and the lower and upper values of the highest probability distribution (HPD) are presented under the three different rates and the respective combined value (see Materials and methods section for details)

Node	Clades	2.0%			1.7%			2.5%			Combined		
		Mean	HPD lower	HPD upper	Mean	HPD lower	HPD upper	Mean	HPD lower	HPD upper	Mean	HPD lower	HPD upper
A	Africa/Europe	11.38	7.49	15.48	13.34	9.03	18.54	9.28	6.59	12.56	11.33	6.43	16.19
B	Betic/Iberia	9.64	5.06	14.85	11.02	5.77	16.65	7.61	4.03	11.66	9.43	4.50	15.14
C	Tunisia/Morocco	8.81	5.35	12.00	10.48	5.96	14.80	7.43	4.57	10.53	8.91	4.73	13.13
D	Rif/Atlas	5.43	3.08	7.83	6.44	3.61	9.40	4.54	2.63	6.79	5.47	2.65	8.18
	Clade L splits	1.93	1.28	2.68	2.39	1.50	3.50	1.58	1.00	2.25	1.97	1.05	3.01

The two main African clades appear to divide the populations into the established species *L. pater* and *L. tangitana*. *L. pater* occurs in Tunisia and part of Algeria (P). The western limits of the clade are unknown due to the lack of sampling inside Algeria. The *L. tangitana* clade (M, T) is distributed in the Atlas and Rifian mountains in Morocco, but extends to the east and beyond the Moulouya river (the northeastern border of Morocco), the classical distribution limit of this species. The eastern limit of this clade inside Algeria is also unknown. There seems to be a discrepancy between the genetic clades and the traditional range of the two species, but it is probable that the traditional limit was assumed to be in accordance to classical biogeographical barriers. The cause of the divergence between the two clades is unknown but the estimated time approximately coincides with the formation of the Tell system and Atlas system II, major orogenic uplifts during the Serravallian–Tortonian ages (de Lamotte *et al.* 2000), or was slightly later. A similar pattern of subdivision in North Africa, but with variable levels of divergence have also been found in other species such as the shrew *Crocidura russula* (Cosson *et al.* 2005), the scorpion *Buthus occitanus* (Gantenbein & Largiader 2003), the lizard *Acanthodactylus erythrurus* (Harris *et al.* 2004) and the terrapins *Mauremys leprosa* (Fritz *et al.* 2006).

Unexpectedly, the Moroccan clade shows further a divergence into two well-differentiated clades. One clade is distributed in the northern part of Morocco, the Rifian mountains and the Moulouya valley (clade T), while the other overlaps the Atlas mountains (clade M), or at least the northern part of it, where the samples were collected, since the remainder of the Atlas was not sampled. However, partial sequences available in GenBank (Table 1, location 39 in Fig. 1) seem to suggest a certain differentiation within clade M (result not shown). Other species such as the chameleon *Chamaeleo chamaeleon* (Paulo *et al.* 2002b), the agamid lizard *Agama impalearis* (Brown *et al.* 2002) and the terrapins *Mauremys leprosa* (Fritz *et al.* 2006) show variable levels of differentiation inside the Morocco area, with an inland-Mediterranean clade and a more coastal-Atlantic clade separated along the Atlas mountain system. This phylogeographical congruence may reflect recurrent process such as climatic changes, which could divide existing populations or lead to the establishment of new ones.

In the European part of the distribution, the age of the main divergence appears to have been close to, or perhaps even older than the main African divergence. The two main European clades are reciprocally monophyletic. Clade N overlaps part of the Betic mountain range and is associated with the subspecies, *Lacerta lepida nevadensis*. Because this clade shows the same level of divergence from the other Iberian clades as that between the two African species and since, additionally, there are some obvious morphological differences, especially in the colour pattern, its upgrade to a full species should be considered.

A particularly important result of this analysis is the association between two well-differentiated clades and the former Miocene islands, i.e. in the Betic mountains (clade N) and the Rif mountains (clade T), and their recent common ancestry with the geographically closest mainland entities on each side of the Mediterranean. However, the range of clade T seems to be more extended than the geographical limits of the Rifian mountains (Fig. 5).

#### *Multiple Iberian Plio–Pleistocene refugia*

The remaining Iberian clades (L1–L4), with much more recent divergence, show a strong association with geographical areas and are reciprocally monophyletic in relation to mtDNA genes. In the case of the  $\beta$ -fibrinogen gene, there is some evidence of paraphyletic group. This difference from the mtDNA pattern might be explained by differential gender migration, in which males have higher dispersal rate, or alternatively by the retention of ancestral polymorphism.

These results corroborate the accumulating evidence for multiple refugia inside the Iberian peninsula, which has now been obtained from several species (e.g. Paulo 2001; Paulo *et al.* 2001; Branco *et al.* 2002; Martinez-Solano *et al.* 2006; Albert *et al.* 2007; Pinho *et al.* 2007). It is particularly interesting to find evidence for multiple Iberian refugia in the ocellated lizard, since it is a typically Mediterranean species. It would appear, then, that suitable conditions persisted in several locations during Plio–Pleistocene glacial maxima. The differentiation between clades appears to have persisted across the successive climatic cycles, even though there are currently no obvious dispersal barriers between them. Similar patterns have been seen in another Iberian lizard species *Lacerta schreiberi* (Paulo 2001; Paulo *et al.* 2002a). Moreover, the genetic evidence suggests that these two species may have shared refugia, in particular the Iberian central mountain system, the northwest/west zone and the southwestern corner of Iberia. These areas may therefore play a more general role in persistence of genetically differentiated forms, and consequently, are of importance for the conservation of biodiversity.

#### *Assessing alternative hypotheses*

The estimated divergence time between African and European lineages refutes the post-MSD vicariance hypothesis, whichever of the mutation rates we used (Table 3). This hypothesis predicted a maximum divergence around 5.33 Ma (it could be slightly higher due to the stochasticity of the genealogical history of each gene), yet even the lowest value of HPD is above 6.4 Ma. Only with an unreasonably high mutation rate, well above 3% per million years, would the genetic divergence coincide with the end of the MSD. Recently Arnold *et al.* (2007) suggested a

divergence between the African–European clades of 8.2 Ma, lower than the values we estimated in this study but within the range of all of our confidence intervals. Calibration differences and the algorithms used could explain the differences in dates obtained in the two studies. However, both divergence dates refute the hypothesis of post-MSD vicariance.

The second hypothesis, of pre-MSD overseas dispersal, was compatible with the estimates for the Euro–African divergence and the divergence between the populations of the former Betic Miocene island and adjacent mainland populations (the Betic/Iberian split), but was not consistent for the Rifian/Atlas divergence. Only with a very fast evolutionary rate would pre-MSD land dispersal explain the divergence of the Betic/Iberian split (7.6 Ma). The Rifian/Atlas split seems to have been initiated during, after or even immediately before MSD. This last scenario is compatible with pre-MSD land dispersal, but only when a slow evolutionary rate is used. However, in any scenario, overseas dispersal seems to explain the divergence of the Betic populations, in contrast to the reconstructed history of the Rifian populations.

Most of these scenarios hold even when the extreme values of the HPD (Table 2) are used. Even the lower values of HPD support pre-MSD dispersal, and all the upper values, but not the lower, support the hypothesis that all Miocene islands were colonized before MSD additionally to pre-MSD dispersal for the African–European split. Only these lower HPD values for each rate, show divergence dates that are not compatible with the scenario of pre-MSD dispersal for the island colonization, but this are extreme, with small associated probabilities.

Vicariance seems to have limited importance in explaining the main evolutionary pattern, although, inside the Iberian Peninsula, vicariance seems instead to have a key role in maintaining the patterns that have become established. Large genetic differences were found between regions or putative refugia, in spite of the similar morphology of the individuals and the absence of any ecological or geographical barriers between them (Paulo 2001). Inside Iberia, the upper limits dated the main events as Pliocene while the lower limits place the main split within the Pleistocene. However, the most probable dates are around the Plio–Pleistocene transition.

However, pre-MSD vicariance as the main process shaping the current phylogeographical pattern of this group, cannot be completely ruled out due to the uncertainty about the geological events that affected this region, and the uncertainty affecting the calibration of the rate of sequence evolution.

Consequently, the original Euro–African split could have been by overland colonization, perhaps followed by a vicariance event that could have occurred in the easternmost part of the species' distribution. These events approximately

coincide with a period of widespread tectonic activity, including the major tectonic deformation phase in the Rifian orogen and the opening of the Tyrrhenian Basin (Azzaroli 1990).

Unlike a number of recently studied species (e.g. Harris *et al.* 2002; Carranza *et al.* 2004; Pinho *et al.* 2006), the ocellated lizards do not appear to have genetic patterns shaped by post-MSL overseas dispersal. However, it should be noted that our sampling was not exhaustive on both sides of the western Mediterranean.

### Final remarks

The calibration of the molecular clock and the estimated phylogeny are central to any description of the biogeographical pattern in the ocellated lizards and discrimination among alternative hypotheses. Because of concerns about the accuracy of the molecular clock for estimating divergence times (Pulquerio & Nichols 2007), we have used relaxed molecular clock models, where the possible variation in evolutionary rates and the uncertainty of their calibration are allowed for.

The established hypothesis for the genetic differentiation of ocellated lizards, the post-MSL vicariance hypothesis, is not supported by our genetic evidence. Instead, it provides strong backing for the alternative hypotheses of pre-MSL overseas dispersal.

Several recent genetic studies of western Mediterranean biogeography have also supported alternatives to post-MSL vicariance – typically suggesting more recent overseas dispersal leading to colonization of vacant similar habitat on the other side of the Mediterranean. Although our results suggested more ancient overseas dispersal, the outcome in either case would be to initiate the divergence between clades, which could eventually lead to different taxonomic entities on either side of the Straits of Gibraltar. Why then do divergence dates not correspond more often with the extraordinary vicariance event when the Mediterranean basin refilled? In the case of the ocellated lizards, it seems that the species were already spread over a wide range and had begun to diverge considerably before the seaway became re-established. In the case of other species, divergence is more likely to have been initiated on the rare occasions when an individual successfully crossed the existing barrier to dispersal to set up a new population.

### Acknowledgements

This work was supported by a Nato Fellowship (Portugal InvoTan, 03/A/97/PO) and by grants from FCT, Portugal and FEDER (POCTI/BSE/48365/2002) to OSP and by the Institute of Zoology, Zoological Society of London. All samples were collected under appropriate licences in each country. We thank Maria Melo, Carlos

Dias, Marta Maymone and António Marcelino for their field work help. We also thank three anonymous referees for their helpful comments.

### References

- Albert EM, Zardoya R, Garcia-Paris M (2007) Phylogeographical and speciation patterns in subterranean worm lizards of the genus *Blanus* (Amphisbaenia: Blanidae). *Molecular Ecology*, **16**, 1519–1531.
- Arnold EN, Arribas O, Carranza S (2007) Systematics of the Palaearctic and Oriental lizard tribe Lacertini (Squamata: Lacertidae: Lacertinae), with descriptions of eight new genera. *Zootaxa* 1430, 1–86.
- Avise JC (2000) *Phylogeography: The History and Formation of Species*. Harvard University Press, Cambridge, Massachusetts.
- Azzaroli A (1990) Paleogeography of terrestrial vertebrates in the perityrrhenian area. *Palaeogeography Palaeoclimatology Palaeoecology*, **77**, 83–90.
- Braga JC, Martin JM, Quesada C (2003) Patterns and average rates of late Neogene – recent uplift of the Betic Cordillera, SE Spain. *Geomorphology*, **50**, 3–26.
- Branco M, Monnerot M, Ferrand N, Templeton AR (2002) Postglacial dispersal of the European rabbit (*Oryctolagus cuniculus*) on the Iberian peninsula reconstructed from nested clade and mismatch analyses of mitochondrial DNA genetic variation. *Evolution*, **56**, 792–803.
- Brown RP, Suarez NM, Pestano J (2002) The Atlas mountains as a biogeographical divide in North-West Africa: evidence from mtDNA evolution in the Agamid lizard *Agama impalearis*. *Molecular Phylogenetics and Evolution*, **24**, 324–332.
- Busack SD (1986) Biogeographic analysis of the herpetofauna separated by the formation of the Strait of Gibraltar. *National Geographic Research*, **2**, 17–36.
- Carranza S, Arnold EN, Wade E, Fahd S (2004) Phylogeography of the false smooth snakes, *Macroprotodon* (Serpentes, Colubridae): mitochondrial DNA sequences show European populations arrived recently from Northwest Africa. *Molecular Phylogenetics and Evolution*, **33**, 523–532.
- Carranza S, Harris DJ, Arnold EN, Batista V, de la Vega JPG (2006) Phylogeography of the lacertid lizard, *Psammotromus algirus*, in Iberia and across the Strait of Gibraltar. *Journal of Biogeography*, **33**, 1279–1288.
- Castroviejo J, Mateo JA (1998) Una nueva subespecie de *Lacerta lepida* Daudin 1802 (Sauria, Lacertidae) para la Isla de Salvora (España). *Publicaciones de la Asociacion de Amigos de Doñana*, **12**, 1–21.
- Cosson JF, Hutterer R, Libois R, Sara M, Taberlet P, Vogel P (2005) Phylogeographical footprints of the Strait of Gibraltar and Quaternary climatic fluctuations in the western Mediterranean: a case study with the greater white-toothed shrew, *Crocidura russula* (Mammalia: Soricidae). *Molecular Ecology*, **14**, 1151–1162.
- Drummond A, Rambaut A (2003) BEAST version 1.4. Available from <http://evolve.zoo.ox.ac.uk/>.
- Drummond AJ, Ho SYW, Phillips MJ, Rambaut A (2006) Relaxed phylogenetics and dating with confidence. *Plos Biology*, **4**, 699–710.
- Duggen S, Hoernle K, van den Bogaard P, Rupke L, Phipps Morgan J (2003) Deep roots of the Messinian salinity crisis. *Nature*, **422**, 602–606.

- Esteban M, Braga JC, Martín JM, Santisteban C (1996) Western Mediterranean reef complexes. In: *Models for Carbonate Stratigraphy from Miocene Reef Complexes of Mediterranean Regions. Concepts in Sedimentology and Paleontology 5* (eds Franseen EK, Esteban M, Ward WC, Rouchy J-M), pp. 55–72. SEPM, Tulsa, Oklahoma.
- Farris JS, Källersjö M, Kluge AG, Bult C (1995) Testing significance of incongruence. *Cladistics*, **10**, 315–319.
- Fritz U, Barata M, Busack SD, Fritzsche G, Castilho R (2006) Impact of mountain chains, sea straits and peripheral populations on genetic and taxonomic structure of a freshwater turtle, *Mauremys leprosa* (Reptilia, Testudines, Geoemydidae). *Zoologica Scripta*, **35**, 97–108.
- Fromhage L, Vences M, Veith M (2004) Testing alternative vicariance scenarios in Western Mediterranean discoglossid frogs. *Molecular Phylogenetics and Evolution*, **31**, 308–322.
- Gantenbein B, Largiadere CR (2003) The phylogeographic importance of the Strait of Gibraltar as a gene flow barrier in terrestrial arthropods: a case study with the scorpion *Buthus occitanus* as model organism. *Molecular Phylogenetics and Evolution*, **28**, 119–130.
- Godinho R, Mendonça B, Crespo EG, Ferrand N (2006) Genealogy of the nuclear beta-fibrinogen locus in a highly structured lizard species: comparison with mtDNA and evidence for intragenic recombination in the hybrid zone. *Heredity*, **96**, 454–463.
- González P, Pinto F, Nogales M, Jiménez-Asensio J, Hernández M, Cabrera VM (1996) Phylogenetic relationships of the Canary Islands endemic lizard genus *Gallotia* (Sauria: Lacertidae), inferred from mitochondrial DNA sequences. *Molecular Phylogenetics and Evolution*, **6**, 63–71.
- Harris DJ, Carranza S, Arnold EN, Pinho C, Ferrand N (2002) Complex biogeographical distribution of genetic variation within *Podarcis* wall lizards across the Strait of Gibraltar. *Journal of Biogeography*, **29**, 1257–1262.
- Harris DJ, Batista V, Carretero MA (2004) Assessment of genetic diversity within *Acanthodactylus erythrurus* (Reptilia: Lacertidae) in Morocco and the Iberian Peninsula using mitochondrial DNA sequence data. *Amphibia-Reptilia*, **25**, 227–232.
- Hsü KJ, Ryan WBF, Cita MB (1973) Late Miocene desiccation of the Mediterranean. *Nature*, **242**, 240–244.
- Huelsenbeck JP, Crandall KA (1997) Phylogeny estimation and hypothesis testing using maximum likelihood. *Annual Review of Ecology and Systematics*, **28**, 437–466.
- Huelsenbeck JP, Larget B, Miller RE, Ronquist F (2002) Potential applications and pitfalls of Bayesian inference of phylogeny. *Systematic Biology*, **51**, 673–688.
- Krijgsman W, Langereis CG (2000) Magnetostratigraphy of the Zozit and Koudiat Zarga sections (Taza-Guercif basin, Morocco): implications for the evolution of the Rifian Corridor. *Marine and Petroleum Geology*, **17**, 359–371.
- Krijgsman W, Hilgen FJ, Raffi I, Sierro FJ, Wilson DS (1999) Chronology, causes and progression of the Messinian salinity crisis. *Nature*, **400**, 652–655.
- Krijgsman W, Garcés M, Agustí J, Raffi I, Taberner C, Zachariasse WJ (2000) The 'Tortonian salinity crisis' of the eastern Betics (Spain). *Earth and Planetary Science Letters*, **181**, 497–511.
- de Lamotte DF, Saint Bezar BA, Bracene R, Mercier E (2000) The two main steps of the Atlas building and geodynamics of the western Mediterranean. *Tectonics*, **19**, 740–761.
- Martin JM, Braga JC, Betzler C (2001) The Messinian Guadalhorce corridor: the last northern, Atlantic–Mediterranean gateway. *Terra Nova*, **13**, 418–424.
- Martinez-Solano I, Teixeira J, Buckley D, Garcia-Paris M (2006) Mitochondrial DNA phylogeography of *Lissotriton boscai* (Caudata, Salamandridae): evidence for old, multiple refugia in an Iberian endemic. *Molecular Ecology*, **15**, 3375–3388.
- Mateo JA, Castroviejo J (1990) Variation morphologique et revision taxonomique de l'espece *Lacerta lepida* Daudin, 1802 (Sauria, Lacertidae). *Bulletin du Muséum de Histoire Naturelle de Paris*, **12**, 691–706.
- Mateo JA, López-Jurado LF, Guillaume CP (1996) Variabilité électrophorétique et morphologique des lézards ocellés (Lacertidae): un complexe d'espèces de part et d'autre du détroit de Gibraltar. *Comptes Rendus de L'Académie des Sciences Serie iii-Sciences de la Vie-Life Sciences*, **319**, 737–746.
- Mateo JA, Santana A, Geniez P (2006) Moroccan ocellated lizard in western Sahara; answer to an old enigma. *Herpetozoa*, **17**, 187–189.
- Nylander JAA (2004) *MRMODELTEST version 2.2*. Program distributed by the author. Evolutionary Biology Centre, Uppsala University.
- Nylander JAA, Ronquist F, Huelsenbeck JP, Nieves-Aldrey JL (2004) Bayesian phylogenetic analysis of combined data. *Systematic Biology*, **53**, 47–67.
- Paulo OS (2001) *The phylogeography of reptiles of the Iberian Peninsula*. PhD Dissertation, University of London.
- Paulo OS, Dias C, Bruford MW, Jordan WC, Nichols RA (2001) The persistence of Pliocene populations through the Pleistocene climatic cycles: evidence from the phylogeography of an Iberian lizard. *Proceedings of the Royal Society B: Biological Sciences*, **268**, 1625–1630.
- Paulo OS, Jordan WC, Bruford MW, Nichols RA (2002a) Using nested clade analysis to assess the history of colonisation and the persistence of populations of an Iberian lizard. *Molecular Ecology*, **11**, 809–819.
- Paulo OS, Pinto I, Bruford MW, Jordan WC, Nichols RA (2002b) The double origin of Iberian peninsular chameleons. *Biological Journal of the Linnean Society*, **75**, 1–7.
- Pinho C, Ferrand N, Harris DJ (2006) Reexamination of the Iberian and North African *Podarcis* (Squamata: Lacertidae) phylogeny based on increased mitochondrial DNA sequencing. *Molecular Phylogenetics and Evolution*, **38**, 266–273.
- Pinho C, Harris DJ, Ferrand N (2007) Contrasting patterns of population subdivision and historical demography in three western Mediterranean lizard species inferred from mitochondrial DNA variation. *Molecular Ecology*, **16**, 1191–1205.
- Posada D, Crandall KA (1998) MODELTEST: testing the model of DNA substitution. *Bioinformatics*, **14**, 817–818.
- Prychitko TM, Moore WS (1997) The utility of DNA sequences of an intron from the beta-fibrinogen gene in phylogenetic analysis of woodpeckers (Aves: Picidae). *Molecular Phylogenetics and Evolution*, **8**, 193–204.
- Pulquerio MJF, Nichols RA (2007) Dates from the molecular clock: how wrong can we be? *Trends in Ecology & Evolution*, **22**, 180–184.
- Rambaut A, Drummond A (2003) *TRACER version 1.0.1*. Available from <http://evolve.zoo.ox.ac.uk/>.
- Ronquist F, Huelsenbeck JP (2003) MRBAYES 3: Bayesian phylogenetic inference under mixed models. *Bioinformatics*, **19**, 1572–1574.
- Shimodaira H, Hasegawa M (1999) Multiple comparisons of log-likelihoods with applications to phylogenetic inference. *Molecular Biology and Evolution*, **16**, 1114–1116.

[Swofford DL \(2000\) PAUP\\*. \*Phylogenetic Analysis Using Parsimony \(\\*and Other Methods\)\*. Version 4.0. Sinauer Associates, Sunderland, Massachusetts.](#)

[Thompson JD, Gibson TJ, Plewniak F, Jeanmougin F, Higgins DG \(1997\) The CLUSTAL\\_X Windows interface: flexible strategies for multiple sequence alignment aided by quality analysis tools. \*Nucleic Acids Research\*, \*\*25\*\*, 4876–4882.](#)

[Thorpe RS, McGregor DP, Cumming AM, Jordan WC \(1994\) DNA evolution and colonization sequence of island lizards in relation to geological history: mtDNA RFLP, cytochrome \*b\*, cytochrome oxidase, 12S rRNA sequence, and nuclear RAPD analysis. \*Evolution\*, \*\*48\*\*, 230–240.](#)

[Veith M, Fromhage L, Kosuch J, Vences M \(2006\) Historical biogeography of Western Palaearctic pelobatid and pelodytid frogs: a molecular phylogenetic perspective. \*Contributions to Zoology\*, \*\*75\*\*, 109–120.](#)

---

Octávio S. Paulo is interested in evolutionary genetics, adaptation and speciation, J. Pinheiro is interested in reptile ecology and A. Miraldo is currently doing a PhD on Hybrid zones. Michael W. Bruford is interested in the evolutionary ecology and population genetics of threatened species. William C. Jordan's interests are in the genetics of adaptiveness. Richard Nichols's research makes use of Bayesian analysis of genetic data to draw inferences about the demography and history of natural populations.

---